

1  
2  
3  
4  
5  
6  
7  
8  
9  
10  
11  
12  
13  
14

**Comparison of soil non-linearity (in situ stress-strain relation and  $G/G_{max}$  reduction) observed  
in strong-motion databases and modelled in ground motion prediction equations**

Philippe Guéguen<sup>1</sup>, Fabian Bonilla<sup>2</sup>, John Douglas<sup>3</sup>

1 ISTERre, Université Grenoble Alpes, CNRS/IFSTTAR – France

2 IFSTTAR, Université Paris Est – France

3 University de Strathclyde, Glasgow – UK

Accepted for publication in the BSSA as a Short Note

15  
16  
17  
18  
19  
20  
21  
22  
23  
24  
25  
26  
27  
28  
29  
30  
31  
32  
33  
34  
35

**Abstract**

Earthquake ground motions are strongly affected by the upper tens of meters of the Earth’s crust and consequently local site effects need to be included in any ground-motion prediction. It is increasingly common in ground motion prediction equations (GMPEs) to account for possible non-linear behavior of near-surface materials (soil). These non-linear site terms adjust observations made on soft soil sites to the ground motion expected on bedrock and hence allow these abundant soil records to be used within the regression analysis for the derivation of empirical GMPEs. These nonlinear site terms also allow rapid predictions of the expected ground motions on soil rather than requiring a site response analysis to be conducted. In this study we compare the signature on observed peak ground acceleration as a function of a strain proxy of non-linear soil behavior within four large strong-motion databases to the predicted signature from four recent GMPEs, three of which explicitly include non-linear site terms. We find that observed non-linearity in the databases, interpreted in terms of strain-stress relationships and reduction of shear modulus, is limited but that even this limited effect is underestimated by the non-linear site terms of the considered GMPEs, which suggests that predictions from these GMPEs could be biased for soft soil sites but also on bedrock. Some of this mismatch could be explained by the use of the average shear-wave velocity in the top 30m ( $V_{s30}$ ) to characterize sites as well as errors in these values.

## 36 **Introduction**

37

38 Ground motion prediction equations (GMPEs) for active crustal regions are generally developed  
39 based on regression analysis of databases of observed strong ground motions (e.g. Douglas and  
40 Edwards, 2016). GMPEs are used in seismic hazard analysis to specify the level of ground motion  
41 expected given variables such as magnitude, distance and basic local site information. Site effects  
42 and their non-linear response are usually considered to be a key element of seismic hazard analysis.  
43 It is widely accepted that non-consolidated sediments tend to behave in a non-linear manner (e.g.,  
44 Field et al., 1997; Bonilla et al., 2005). The non-linear response of superficial soil layers is  
45 characterized by a reduction in the high-frequency amplification, related to an increase of damping,  
46 and the shifting of the resonance frequency to lower frequencies, due to a reduction of the shear  
47 modulus,  $G$  (e.g., Assimaki et al., 2008; Bonilla et al., 2005; Régnier et al., 2013).

48

49 Terms associated with non-linear response of soils have recently been introduced into GMPEs (e.g.,  
50 Abrahamson et al., 2014; Boore et al., 2014; Akkar et al., 2014). Uncertainties related to site effects  
51 make a significant contribution to the total uncertainties of these equations, and therefore to seismic  
52 hazard studies (Bommer and Abrahamson, 2006; Rodriguez-Marek et al., 2011). In particular, the use  
53 of *in situ* geophysical surveys to characterize the elastic properties and laboratory tests to assess the  
54 non-linear behavior parameters may result in estimation bias, affecting the GMPEs (e.g., Cabas et al.,  
55 2017). This bias may be due to differences between *in situ* and laboratory conditions, the presence of  
56 superficial layers with a significant effect (Régnier et al., 2013) or even three-dimensional geometric  
57 effects that cannot be replicated in the laboratory (e.g., Frankel et al., 2002; Assimaki et al., 2008;  
58 Sleep, 2010). In addition, the strong-motion data affected by strong soil non-linearity appeared to be  
59 insufficient in the international databases for completely empirical non-linear soil terms, which  
60 demands the use of modelling to develop such terms (e.g., Akkar et al., 2014, Zhao et al., 2015).

61

62 Thanks to recent efforts to install dense strong-motion networks and characterize local site conditions  
63 at these stations, it is now possible to interpret non-linearity *in situ* by analyzing the recorded data.  
64 The variation of  $G$  has thus been obtained from borehole data (Frankel, 1999) by measuring the  
65 velocity variation as a function of shear deformation by intercorrelation (e.g., Rubinstein and Beroza,  
66 2005) and by seismic interferometry (Sawazaki et al., 2009; Chandra et al 2015, 2016; Guéguen,  
67 2016). This shear strain can be calculated using a deformation proxy linking the medium's shear-  
68 wave velocity  $V_s$  to the maximum particle velocity, which is generally equivalent to the peak ground  
69 velocity,  $PGV$  as  $PGV/V_s$  (Rathje et al. 2004; Idriss, 2011). Furthermore, the peak ground acceleration  
70 ( $PGA$ ) at the top of the soil column is a proxy of shear stress and the  $PGA$  versus  $PGV/V_s$ , and even  
71  $PGA$  versus  $PGV/V_{s30}$  relationships can be associated with a stress-strain curve, i.e. an *in situ* test  
72 comparable with laboratory tests to reproduce non-linear effects (Chandra et al., 2015, 2016).

73  
74 The purpose of this study is, therefore, to characterize the non-linear parameters, interpreted in terms  
75 of strain-stress relationships and reduction of shear modulus, using the international databases from  
76 which the GMPEs are derived. These parameters will be presented in the first part. In the second part,  
77 we will present the data used in this study, taken from four international databases. A final section  
78 presents a comparison of the data interpreted as strain-stress relationships, with the non-linear soil  
79 terms present in a selection of GMPEs.

80

### 81 ***In situ* stress and strain proxies**

82

83 In the linear elastic domain, the relationship between shear strain and stress is directly proportional  
84 to  $G_{max}$ , i.e.

85

$$86 \quad \tau = G_{max} \gamma \quad (1)$$

87

88 where  $\tau$  is the shear stress,  $\gamma$  is the shear deformation and  $G_{max}$  is the elastic shear modulus, i.e. the  
89 value under slight deformation. In the nonlinear domain, soil behavior is traditionally modelled by  
90 the following hyperbolic nonlinear model (Ishihara, 1996):

91

$$92 \quad \tau = \frac{G_{max} \gamma}{1 + \gamma/\gamma_r} \quad (2)$$

93

94 with  $\gamma_r$  being the reference deformation and defined as  $G_{max}/\tau_{max}$ , where  $\tau_{max}$  is the maximum  
95 strength of the material. Assuming the propagation of a unidirectional wave in an infinitely uniformly  
96 elastic medium, the shear strain is considered according to the following equation (Newmark, 1968):

97

$$98 \quad \gamma = V_{max}/\beta \quad (3)$$

99

100 where  $V_{max}$  is the maximum particle velocity and  $\beta$  the apparent velocity of the shear waves, i.e.,  
101  $\beta = \sqrt{G_{max}/\rho}$  where  $\rho$  is density. Considering maximum horizontal acceleration proportional to the  
102 shear stress ( $\tau$ ) and the strain according to Eq. 3, Chandra et al. (2015, 2016) used data from a vertical  
103 array to evaluate the variation of  $\beta$  (and therefore of  $G$ ) according to the strain calculated between  
104 two sensors during seismic loading. They thus derived an *in situ* model of the nonlinear behavior of  
105 soil based on an interpretation of the experimental data in terms of strain-stress values, equivalent to  
106 the hyperbolic model (Eq. 2). On the basis of Eq. 3, Idriss (2011) suggested considering  $PGV/V_{s30}$   
107 as the average strain over the first 30m, where nonlinearity is mainly expected to occur,  $PGV$  being  
108 comparable to  $V_{max}$  in Eq.3. Finally, by considering the shear stress proportional to acceleration and  
109  $PGA$  (i.e.,  $\tau = PGA \times h \times \rho$ , with  $h$  the equivalent depth), Chandra et al. (2016) confirmed the  
110 possibility of distinguishing the average behavior of different site classes (classed according to  $V_{s30}$ )  
111 according to a strain proxy, i.e.  $PGA = f(PGV/V_{s30})$ , using data from the Japanese networks KNET  
112 and KiK-net.

113

114 From Eq. 1, we thus obtain the *in situ* stress-strain relationship under elastic deformation, as follows:

115

$$116 \quad PGA = G_{max} \cdot PGV/V_{s30}/h/\rho \quad (4)$$

117

118 i.e., the maximum shear stress proxy is proportional to  $PGA$  and the shear strain proxy to  $PGV/V_{s30}$ ,

119 i.e.  $G$  is proportional to  $PGA/(PGV/V_{s30})$ . We can then obtain an experimental *in situ* curve

120 characterizing the nonlinear behavior by the reduction of modulus  $G$  according to the following

121 equation:

122

$$123 \quad \frac{G}{G_{max}} = \frac{PGA}{PGV/V_{s30}} / \left( \frac{PGA}{PGV/V_{s30}} \right)_{max} \quad (5)$$

124

125 where  $\left( \frac{PGA}{PGV/V_{s30}} \right)_{max}$  is computed for  $PGV/V_{s30} < 10^{-5}\%$  corresponding to the linear elastic

126 deformation limit (Vucetic, 1994; Johnson and Jia, 2005). Using *in situ* data, we can then explore the

127 nonlinearity in strong-motion databases, evaluated using the shear strain proxy (Eq. 3) and the shear

128 modulus reduction (Eq. 5). In our case, the nonlinearity is associated with the reduction of modulus

129  $G$ , and this reduction can be predicted or calculated using GMPEs (Eq. 5).

130

## 131 **Database description**

132

133 Four databases were used to test the nonlinear parameters in the data, only taking into account the

134 parameters required for Eq. 5 as well as earthquake magnitude: the intensity measures considered

135 were  $PGA$  and  $PGV$  and the site parameter was the  $V_{s30}$ . Data processing and information describing

136 the source of these data are described in the original papers and the flat files.

137

138 - NGA-West2 flat file provided by *Pacific Earthquake Engineering Research Center* (Ancheta  
139 et al., 2014). The file contains 21,540 ground motion records, recorded during shallow crustal

140 earthquakes in active tectonic regions worldwide. Two types of  $V_{s30}$  values are distinguished  
141 in this database, estimated or direct measurement, which will be discussed later.

142

143 - K-NET and KiK-net Japanese network databases (Okada et al., 2004), characterized by two  
144 different types of installations (Aoi et al., 2004). One of the advantages of the Japanese  
145 networks is the homogeneity of the metadata, characterizing the earthquakes (e.g. magnitude  
146 and locations) and the local site conditions. For K-NET, measurements were taken up to a  
147 depth of 20m, and  $V_{s30}$  was then estimated using KiK-net velocity surveys that go deeper  
148 (Boore et al., 2011). For KiK-net,  $V_{s30}$  was calculated directly from velocity profiles going  
149 from 100 up to 2008 m. For this study, K-NET records having a PGA larger than  $10 \text{ cm/s}^2$   
150 were collected between 1996 and end of 2016, irrespective of distance or magnitude. We use  
151 the KiK-net data processed by Regnier et al. (2013), consisting the records between 1996 and  
152 2009, with magnitudes higher than 3 and a hypocentral depths and epicentral distances less  
153 than 150 km. We also added data from the mainshock and aftershocks of the  $M_w$  9.0 Tohoku  
154 2011 earthquake. Finally, we completed this database with records having PGAs larger than  
155  $100 \text{ cm/s}^2$  up to the end of 2016. Data processing is described in Régnier et al. (2013) and  
156 Laurendeau et al. (2013). We used a total of 178,556 records from KiK-net and 26,895 from  
157 K-NET.

158

159 - ESM (Engineering Strong-Motion) database (Luzi et al., 2016) containing data from the  
160 European networks was the final source of data. ESM was developed as part of the European  
161 NERA project, and was designed to provide end users with data from moderate and strong  
162 earthquakes in the European and Mediterranean region. The data has been quality-checked  
163 and uniformly processed, and relevant parameters, from 1969 to the present day. The 2017  
164 flat-file was produced for the EPOS project and provided directly by the ESM facility. The  
165 ESM flat-file contains a total of 3,434 records.

166

167 The distribution of the data used in this study according to PGA and strain proxy (Eq. 4) is shown in  
168 Fig. 1 for the different databases separately. The ESM and NGA-West2 databases contain the lowest  
169 strain proxies. The ranges of  $PGA$  and  $PGV/V_{s30}$  are broader for NGA-West2, with many values above  
170  $1 \text{ m/s}^2$  for  $PGA$  and  $0.1\%$  for the strain proxy. A large number of strain proxies are below  $10^{-4}\%$ , i.e.  
171 below the linear cyclic deformation threshold (Vucetic, 1994) determined from laboratory tests.  
172 Between the linear ( $10^{-4}\%$ ) and volumetric ( $10^{-2}\%$ ) strain thresholds (Vucetic, 1994), the soil  
173 displays nonlinear elastic behavior with negligible permanent deformation. Above  $10^{-2}\%$ , the soil  
174 shows hysteretic nonlinear behavior with permanent deformation. Considering the data from the four  
175 databases, some must therefore contain nonlinear processes according to the soil models based on  
176 laboratory tests. The best-fit (linear) equations are similar, with similar slopes for three databases  
177 (ESM, KiK-Net and NGA-West2). It is also interesting to note that the coefficient of correlation  $R^2$   
178 for these three databases are quite high ( $>0.5$ ) and suggest that these three databases are comparable  
179 and will all reproduce the equivalent strain-stress relationships. For the KNET data, however,  $R^2$  is  
180 quite low (0.139) in the log-log representation, which suggests a poor prediction of the data by simple  
181 linear regression, suggesting an additional physical reason that we speculate is the presence of soil  
182 nonlinearities in the data. The nonlinearities in KNET data was also reported by Chandra et al. (2016),  
183 when comparing KiK-Net and KNET, who conclude that the KNET data shows the highest  
184 nonlinearity. Assuming higher nonlinearity in the KNET data, it is interesting to observe that these  
185 nonlinearities are for lower values of  $PGA$ , suggesting the inefficiency of  $PGA$  for the prediction of  
186 soil nonlinearity.

187

188

189 **Nonlinear characterization**

190



191 The nonlinearity observed in the databases selected for this study was assessed using Eq. 5. In our  
192 case,  $\left(PGA/\frac{PGV}{V_{s30}}\right)_{max}$  was considered as the average of the values lower than  $10^{-5}$  %. For KNET and  
193 the lowest values of  $V_{s30}$ , because of more data showing nonlinearity, the smallest values already  
194 contain nonlinearities and the plot is biased at low strain proxies. Since nonlinearity is highly  
195 dependent on site conditions, we separated the data according to  $V_{s30}$ , into three categories: [100-  
196 300]m/s, [400-600]m/s and [800-1,200]m/s, i.e. the approximate conditions C, B and A of Eurocode  
197 8, respectively, in order to compare soils with *a priori* different nonlinear behavior. Fig. 2 shows the  
198 nonlinearity representation for the four databases. Means and standard deviations are indicated for  
199 different strain range values using a logarithmic scale (in %): [ $<10^{-6}$ ], [ $10^{-6} - 3.5 \cdot 10^{-6}$ ], [ $3.5 \cdot 10^{-6} - 1.2$   
200  $10^{-5}$ ], [ $1.2 \cdot 10^{-5} - 4.3 \cdot 10^{-5}$ ], [ $4.3 \cdot 10^{-5} - 1.5 \cdot 10^{-4}$ ], [ $1.5 \cdot 10^{-4} - 5.3 \cdot 10^{-4}$ ], [ $5.3 \cdot 10^{-4} - 1.9 \cdot 10^{-3}$ ], [ $1.9 \cdot 10^{-3} - 6.6$   
201  $10^{-3}$ ], [ $6.6 \cdot 10^{-3} - 2.3 \cdot 10^{-2}$ ], [ $2.3 \cdot 10^{-2} - 8.1 \cdot 10^{-2}$ ], [ $8.1 \cdot 10^{-2} - 2.8 \cdot 10^{-1}$ ] and [ $2.8 \cdot 10^{-1} - 1$ ].

202

203 We can see that, in spite of the large amount of data from various sources, nonlinearity characterized  
204 by the  $G/G_{max}$  reduction, is barely visible compared to the 95% and 90% reduction values of  $G/G_{max}$   
205 in Figures 2a and 2b. This raises questions on whether nonlinearity can be incorporated empirically  
206 into GMPEs, particularly as its first effect is to reduce ground motion by increasing the energy  
207 dissipation. We also observe a slight dependency on magnitude. As expected, the decrease of  $G/G_{max}$   
208 is greatest for the largest magnitudes, but for a given strain proxy, the range of magnitude values and  
209  $G/G_{max}$  values is broad, regardless of  $V_{s30}$ .

210

211 For the lowest  $V_{s30}$  values, nonlinearity characterized by the variation in  $G/G_{max}$  makes a significant  
212 appearance at a strain proxy threshold of approximately  $5 \cdot 10^{-4}$  % for the Japanese data and  $10^{-3}$  % in  
213 ESM and NGA-West2, with reduction of  $G/G_{max}$  larger than 90%. For the intermediary  $V_{s30}$  values,  
214 nonlinearity appears at around  $10^{-3}$  % while for the highest  $V_{s30}$  values, a  $G$  reduction is visible from  
215  $5 \cdot 10^{-3}$  % to  $10^{-2}$  % for Japanese and other databases, respectively, i.e. nonlinear effects may also  
216 appear in stiff soils. However, care must be taken when classifying sites on the basis of  $V_{s30}$ , as certain

217 recent studies have demonstrated visible nonlinear effects for sites with a  $V_{s30}$  greater than 800m/s  
218 but with a thin surface layer sensitive to nonlinearity (Bonilla et al., 2011; Régnier et al., 2013).

219

220

## 221 **Integrating non-linearity in the GMPEs**

222

223 Several GMPEs include site terms accounting for soil nonlinearity. We selected four recent GMPEs:  
224 Akkar et al. (2014), Boore et al., (2014) and Abrahamson et al. (2014) that include nonlinear site  
225 terms and Bindi et al. (2014) as reference with linear site terms. These four GMPEs provide  
226 predictions of  $PGA$  and  $PGV$  as a function of magnitude and source-to-site distance, and for different  
227 site conditions. Fig. 3 shows  $PGA$  predictions as a function of the strain proxy  $PGV/V_{s30}$ . The  
228 predictions are for magnitudes between 4 and 8 (0.5 intervals) and 50 distances logarithmically spaced  
229 between 0.1 and 300km. This unusual manner of representing ground-motion predictions as a  
230 function of strain proxy, enables visualization of how nonlinearity, interpreted as the reduction of  $G$   
231 with respect to the strain proxy, is integrated in the GMPEs. It should be noted that the regression  
232 analysis used to derive each GMPE was conducted independently for  $PGA$  and  $PGV$  with different  
233 nonlinear site terms assumed for each. Also many scenarios where large  $PGAs$  and  $PGVs$  occur ( $M > 7$   
234 and  $R < 20\text{km}$ ), and consequently there is a high chance of soil nonlinearity, are poorly sampled in the  
235 strong-motion databases, especially at soft soil sites. Therefore, the predictions from the GMPEs are  
236 more uncertain for these scenarios and depend strongly on the functional form adopted by the GMPE  
237 developer rather than being strongly constrained by the data.

238

239 As expected, nonlinearity is more present for soft soils ( $V_{s30}=100\text{m/s}$ ) than for stiff soils  
240 ( $V_{s30}=1,000\text{m/s}$ ), with an equivalent stress (i.e.,  $PGA$ ) - strain (i.e.  $PGV/V_{s30}$ ) relationship that changes  
241 as deformation increases. The differences with the linear Bindi et al. (2014) GMPE are larger for soft  
242 site conditions.

243

244 We observe that the three GMPEs of Akkar et al. (2014), Boore et al. (2014) and Abrahamson et al.  
245 (2014) integrate nonlinearity differently and that using a GMPE with a linear site term (e.g. Bindi et  
246 al., 2014) may introduce a significant bias in terms of stress-strain proxies compared to previous  
247 prediction models for soft soils ( $V_{s30}=100$  m/s or 200m/s). The curvature of the prediction increasing  
248 with strain proxy characterizes the nonlinearity accounted for by the GMPEs. Abrahamson et al.  
249 (2014) characterizes nonlinearity more strongly for soft ( $V_{s30}=100$ m/s) and intermediate soils  
250 ( $V_{s30}=200$ m/s) than Boore et al. (2014) and Akkar et al. (2014). The differences between nonlinear  
251 models challenges the way in which GMPEs consider nonlinear effects, leading to *PGAs* that are  
252 significantly different for the same magnitude-distance pairs. For example, compared to Bindi et al.  
253 (2014), the curvature of Boore et al. (2014) and Akkar et al. (2014) is not significant and the  
254 nonlinearity is considered as reducing the ground motion for equivalent strain values. These models  
255 principally use results taken from numerical modelling. This dispersion shows the high epistemic  
256 uncertainty in predicted ground motions, considering strain proxy and the G reduction, for soft soils  
257 undergoing high deformations. Nonlinear site terms in GMPEs are often introduced so that observed  
258 ground motions from soft soil sites can be reliably used, by removal of the site effects, to derive  
259 models to assess ground motions on bedrock. The ground motions implied by seismic hazard  
260 assessment using these GMPEs evaluated for bedrock conditions are subsequently used to select rock  
261 strong-motion records for input to site response analysis.

262

263 Figure 4 compares the predictions of the proxies of  $G/G_{max}$  according to the strain proxies from the  
264 four GMPEs considered in this study with the average values taken from the databases for three site  
265 classes (the class  $V_{s30}<100$ m/s is not considered because of insufficient data).

266

267 Several observations can be made from Fig. 4.

268

269 (1) Firstly, as expected, nonlinearity is more obvious for soils  $100 < V_{s30} < 300$  m/s, characterized by  
270 larger shear strain proxy, which confirms that the  $PGA$  versus  $PGV/V_{s30}$  relationship is an efficient  
271 proxy to characterize the nonlinear *in situ* behavior of soil. These proxies and the scattering of the  
272 relationships could be reduced by integrating the occurrence time of the maximum values of  
273 acceleration, velocity and displacement (deformation) that may not occur at the same time, as  
274 suggested by Chandra et al. (2016) and Guéguen (2016).

275  
276 (2) Based on the  $G/G_{max}$  reduction factor (with respect to the 95 and 90% thresholds), the ESM data  
277 seems to indicate less nonlinearity for soft soils than the other databases, particularly compared with  
278 the Japanese sites, which we know show clear nonlinear behavior (Régnier et al., 2013). However,  
279 this observation could be modulated according to the larger dispersion of the ESM data. The KNET  
280 stations show more marked nonlinear behavior than the KiK-net stations, which is in agreement with  
281 observations already reported by other authors (Aoi et al., 2004; Chandra et al., 2016) who concluded  
282 on a more pronounced nonlinear behavior for KNET than for KiK-net data, as a consequence of soil  
283 profiles beneath their stations.

284  
285 (3) Compared with soil behavior based on laboratory tests and characterized by a traditional  $G - \gamma$   
286 curve, it appears that nonlinearity is limited, in spite of the large spread of data in international  
287 databases in terms of magnitude and distance, with the modulus  $G/G_{max}$  reduction only reaching 30%  
288 in the worst case for the sites most sensitive to nonlinearity ( $100 < V_{s30} < 300$  m/s). This observation  
289 suggests that nonlinearity effects are rare in the global databases used herein. Since the databases  
290 used in this study represent a significant proportion of strong-motion data ever recorded, this  
291 observation makes us wonder whether large ( $>1$  %) strains could be expected during earthquakes. It  
292 also raises the question of considering nonlinearity, using modelling techniques or laboratory results,  
293 to define seismic demand, since site response may be underestimated compared to the observation.  
294 Perus and Fajfar (2014) proposed site factors between ground motions on sites characterized by low

295  $V_{s30}$  and those on rock sites that overestimate the nonlinear effects in the predicting ground motion.  
296 In Perus and Fajfar (2014) few data are used and their conclusions are based on predicted values of  
297 PGA or  $S_a$ , and consequently, they recommend a careful consideration of their results since strong-  
298 motion data enable a better consideration of nonlinearity. In our study, and based on the variation of  
299  $G/G_{max}$ , we observe a small effect of nonlinearities in predictions and observations, even for  
300  $V_{s30}<300\text{m/s}$ , in contrast to Perus and Fajfar (2014). Chandra et al (2016) also suggested the limited  
301 effect of nonlinearities in the Japanese databases, with average accelerations on soil sites comparable  
302 to rock sites values, even for  $\text{PGA}>0.2\text{g}$ . In our study, even if GMPEs underestimate the nonlinear  
303 effects, they are very comparable to the nonlinearity contained in the database.

304

305 (4) The  $G/G_{max}$  versus  $PGV/V_{s30}$  relationship is comparable for the four databases, independently  
306 of the magnitude-distance relationship. Using the terminology of Luco and Cornell (2007) for an  
307 intensity measure of ground motion, this proxy is “efficient” for nonlinearity characterization. Fig. 5  
308 shows shear strain proxy as a function of magnitude. Fig. 5 reveals that magnitude does not control  
309 the appearance of nonlinearity, if the latter is characterized according to shear strain proxy,  
310 confirming the representativeness of magnitude-distance criteria for predicting nonlinearity.

311

312 (5) The predictions of soil nonlinearity from the GMPEs are similar overall: underestimating the  $G$   
313 reduction compared with the data. They are generally based on simulation techniques and do not  
314 represent the nonlinearity that can be observed in the databases. It is also interesting to observe that  
315 Bindi et al (2014) shows an increase in the curvature for the largest strains. This suggests that this  
316 GMPE implicitly includes some soil nonlinearity in its predictions, due to the underlying data, despite  
317 using linear site terms, or that various GMPE terms (such as those related to the site amplification)  
318 are not fully independent. This point could be confirmed by numerical simulation or more specific  
319 analysis of this database.

320

321 (6) For the  $800 < V_{s30} < 1,200$  m/s class, the data from NGA-West2 display more non-linear behavior  
322 than those of the other databases. It is important to remember that certain  $V_{s30}$  values are possibly  
323 underestimated or not measured in the NGA-West2 database. Fig. 6 shows the reduction in  $G$  for  
324 NGA-West2, distinguishing between the sites with measured  $V_{s30}$  and the sites with estimated  $V_{s30}$ .  
325 A readjustment of the data to the GMPE predictions is observed for all site conditions, but particularly  
326 for stiff soil sites ( $800 < V_{s30} < 1,200$  m/s). This leads us to conclude that certain  $V_{s30}$  estimates are not  
327 correct in NGA-West2 meaning that some sites are incorrectly classified here.

328

329 This random 10% variation of the  $V_{s30}$  values for the  $800 < V_{s30} < 1,200$  m/s class enables observation  
330 of the strong sensitivity of the nonlinearity to this parameter. We can, therefore, conclude that the  
331 consideration of nonlinearity requires detailed and precise characterization of site conditions, already  
332 mentioned for the prediction of ground motion, but all the more important if we intend to include  
333 nonlinear site terms in the equations.

334

## 335 **Conclusions**

336 In this project, we analyzed strong-motion data from four large databases worldwide. These data are  
337 often used by researchers to derive GMPEs, which are used to estimate earthquake ground motions  
338 for a given magnitude and source-to-site distance. Although these equations are useful for prediction  
339 of ground motions on rock, they are less efficient for prediction on soil, particularly for  $V_{s30} < 300$  m/s,  
340 which reflects the sparsity of the data for this range of  $V_{s30}$  (Ktenidou et al., 2018). Indeed, such soils  
341 may display a nonlinear response due to their low resistance and a strong incident motion, as is the  
342 case for sites close to the seismic source or with strong amplification. To take such behavior into  
343 account, GMPEs have been modified to include the shear modulus reduction according to strain proxy.  
344 Description of the soil's nonlinear behavior used for numerical modeling is based on a few parameters,  
345 mainly obtained by laboratory tests, which do not represent the natural variability of soils and which  
346 neglect the propagation effects of seismic waves in the medium.

347 We found the characterization of  $V_{s30}$  to be essential to good prediction of the non-linear response.  
348 Soil nonlinearity, interpreted in terms of  $G$  reduction for given strain proxy values, exists and is  
349 stronger than that predicted by the GMPEs. However, unlike in the geotechnical models based on  
350 laboratory tests, the shear deformation observed in the international databases remains low, limited  
351 to a shear modulus reduction of around 30% for the softest soils. The comparison between  
352 geotechnical model and in-situ observation could be compared through numerical modeling in further  
353 studies. In addition, reduction in  $G$  with increasing strain proxy in stiff soils was also observed, which  
354 may be due to thin superficial layers that cause nonlinearity as already supported by Régnier et al.  
355 (2013) for Japanese data.

356

### 357 **Acknowledgements**

358 This project was partially funded by the French accelerometric network programme, within the  
359 framework of its 2017 Call of Proposal. The authors would like to thank the data providers enabling  
360 the compilation of the information in the flat-files. This study is part of the Urban Seismology project  
361 of the Earth Sciences Institute (Université Grenoble Alpes), and was supported by funding from  
362 Labex OSUG@2020 (Investissements d'avenir, ANR10-LABX56). We thank Fabrice Cotton and an  
363 anonymous reviewer for their careful and useful comments on an earlier version of this study.

### 364 **Data and Resources**

365 Authors used the technical resources provided by the French Accelerometric Network database  
366 (RAP-DC, doi:10.15778/RESIF.RA <http://data.datacite.org/10.15778/RESIF.RA>) for processing the  
367 data. Flat-files of strong motion database were downloaded from European Strong Motion (ESM)  
368 flat-file <http://esm.mi.ingv.it/flatfile-2017/flatfile.php>) and Pacific Earthquake Engineering Research  
369 (PEER) ground-motion database (<http://peer.berkeley.edu/ngawest2/>) (last access: June 2018). K-  
370 NET and KiK-Net flat files were provided by references cited in the manuscript, using data  
371 downloaded from the strong-motion seismograph network services operated by the National Research

372 Institute for Earth Science and Disaster Resilience (NIED) seismological services  
373 (<http://www.kyoshin.bosai.go.jp/>).

## 374 **References**

375

376 Abrahamson, N. A., W. J. Silva, R. and Kamai (2014). Summary of the ASK14 ground motion  
377 relation for active crustal regions, *Earthquake Spectra* **30(3)** 1025-1055.

378

379 Akkar, S., M. A. Sandıkkaya, and J. J. Bommer (2014). Empirical ground-motion models for point-  
380 and extended-source crustal earthquake scenarios in Europe and the Middle East, *Bulletin of*  
381 *Earthquake Engineering* **12(1)** 359-387.

382

383 Ancheta, T. D., R. B. Darragh, J. P. Stewart, E. Seyhan, W. J. Silva, B.S.-J. Chiou, K. E. Wooddell,  
384 R. W. Graves, A. R. Kottke, D. M. Boore, T. Kishida, and J. L. Donahue (2014). NGA-West2  
385 database, *Earthquake Spectra* **30** 989– 1005.

386

387 Aoi S., T. Kunugi, and H. Fujiwara (2004). Strong-motion seismograph net-work operated by NIED:  
388 K-NET and KiK-net, *J. Jpn Assoc. Earthq. Eng.* **4(3)** 65–74.

389

390 Assimaki, D., W. Li, J. H. Steidl, and K. Tsuda (2008). Site amplification and attenuation via  
391 downhole array seismogram inversion: A comparative study of the 2003 Miyagi-Oki aftershock  
392 sequence, *Bull. Seism. Soc. Am.* **98(1)** 301-330.

393

394 Bindi, D., M. Massa, L. Luzi, G. Ameri, F. Pacor, R. Puglia, and P. Augliera (2014). Pan-European  
395 ground-motion prediction equations for the average horizontal component of PGA, PGV, and 5%-  
396 damped PSA at spectral periods up to 3.0 s using the RESORCE dataset, *Bulletin of Earthquake*  
397 *Engineering* **12(1)** 391-430.



398

399 Bommer, J. J., and N. A. Abrahamson (2006). Why do modern probabilistic seismic-hazard analyses  
400 often lead to increased hazard estimates?, *Bull. Seism. Soc. Am.* **96(6)** 1967-1977.

401 Bonilla, L. F., R. J. Archuleta, and D. Lavallée (2005). Hysteretic and dilatant behavior of  
402 cohesionless soils and their effects on nonlinear site response: field data observations and modeling,  
403 *Bull. Seism. Soc. Am.* **95** 2373-2395.

404 Bonilla L.F., K. Tsuda, N. Pulido, J. Régnier, and A. Laurendeau (2011). Nonlinear site response  
405 evidence of K-NET and KiK-net records from the 2011 off the Pacific coast of Tohoku Earthquake,  
406 *Earth Planets Space* **63** 785–789.

407 Boore, D., E. Thompson, and H. Cadet (2011). Regional correlations of VS30 and velocities averaged  
408 over depths less than and greater than 30 meters, *Bull. Seism. Soc. Am.* **101(6)** 3046–3059.

409 Boore, D. M., J. P. Stewart, E. Seyhan, and G. M. Atkinson (2014). NGA-West2 equations for  
410 predicting PGA, PGV, and 5% damped PSA for shallow crustal earthquakes, *Earthquake Spectra*  
411 **30(3)** 1057-1085.

412

413 Cabas, A., A. Rodriguez-Marek, and L. F. Bonilla (2017). Estimation of site-specific Kappa (K0)-  
414 consistent damping values at KiK-Net sites to assess the discrepancy between laboratory-based  
415 damping models and observed attenuation (of seismic waves) in the field, *Bull. Seism. Soc. Am.*  
416 **107(5)** 2258-2271.

417

418 Chandra, J., P. Guéguen, J. H. Steidl, and L. F. Bonilla (2015). In situ assessment of the G– $\gamma$  curve  
419 for characterizing the nonlinear response of soil: Application to the Garner Valley downhole array  
420 and the wildlife liquefaction array, *Bull. Seism. Soc. Am.* **105(2A)** 993-1010.

421

422 Chandra, J., P. Guéguen, P., and L. F. Bonilla (2016). PGA-PGV/Vs considered as a stress–strain  
423 proxy for predicting nonlinear soil response, *Soil Dynamics and Earthquake Engineering* **85** 146-160.  
424

425 Douglas, J. and B. Edwards (2016). Recent and future developments in earthquake ground motion  
426 estimation, *Earth-Science Reviews* **160** 203-219.  
427

428 Field, E. H., P. A. Johnson, I. A. Beresnev, and Y. Zeng (1997). Nonlinear ground-motion  
429 amplification by sediments during the 1994 Northridge earthquake, *Nature* **390(6660)**, 599.  
430

431 Frankel, A. D. (1999). How does the ground shake?, *Science* **283(5410)** 2032-2033.  
432

433 Frankel, A. D., D. L. Carver, and R. A. Williams (2002). Nonlinear and linear site response and basin  
434 effects in Seattle for the M 6.8 Nisqually, Washington, earthquake, *Bull. Seism. Soc. Am.* **92(6)** 2090-  
435 2109.  
436

437 Guéguen, P. (2016). Predicting nonlinear site response using spectral acceleration vs PGV/Vs30: a  
438 case history using the Volvi-test site, *Pure and Applied Geophysics* **173(6)** 2047-2063.  
439

440 Idriss, I.M. (2011). Use of Vs30 to represent local site condition, in *Proc. 4th IASPEI/ IAEE*  
441 *International Symposium. Effects of Source Geology on Seismic Motion*. August 23-26th, 2011.  
442 University of Santa Barbara California.  
443

444 Ishihara K. (1996). *Soil behaviour in earthquake geotechnics*. Oxford Engineering Science Series.  
445 Oxford University Press.  
446

447 Johnson, P. A., and X. P. Jia (2005). Nonlinear dynamics, granular media and dynamic earthquake

448 triggering, *Nature* **437** 871–874.

449

450 Ktenidou, O. J., Z. Roumelioti, N. Abrahamson, F. Cotton, K. Pitilakis, and F. Hollender (2018).  
451 Understanding single-station ground motion variability and uncertainty (sigma): lessons learnt from  
452 EUROSEISTEST, *Bulletin of Earthquake Engineering* **16(6)** 2311-2336.

453

454 Laurendeau A., F. Cotton, O.-J. Ktenidou, L. F. Bonilla, and F. Hollender (2013). Rock and stiff-soil  
455 site amplification: dependency on Vs30 and Kappa ( $\kappa_0$ ), *Bull. Seism. Soc. Am.* **103(6)** 3131–48.

456

457 Luco, N. and C. A. Cornell (2007). Structure-specific scalar intensity measures for near-source and  
458 ordinary earthquake ground motions, *Earthquake Spectra* **23(2)** 357-392.

459

460 Luzi L., R. Puglia, E. Russo, M. D'Amico, C. Felicetta, F. Pacor, G. Lanzano, U. Ceken, J. Clinton,  
461 G. Costa, L. Duni, E. Farzanegan, P. Guéguen, C. Ionescu, I. Kalogeras, H. Özener, D. Pesaresi, R.  
462 Sleeman., A. Strollo, and M. Zare (2016). The engineering strong-motion database: A platform to  
463 access pan-European accelerometric data, *Seismological Research Letters* **87(4)** 987-997.

464

465 Newmark, N.M. (1968). Problems in Wave Propagation in Soil and Rock, In *Symposium on Wave*  
466 *Propagation and Dynamic Properties of Earth Materials*, August 23-25, Univ. of New Mexico Press,  
467 Albuquerque, NM, 7-26.

468

469 Okada, Y., K. Kasahara, S. Hori, K. Obara, S. Sekiguchi, H. Fujiwara, and A. Yamamoto (2004).  
470 Recent progress of seismic observation networks in Japan—Hi-net, F-net, K-NET and KiK-net,  
471 *Earth, Planets and Space* **56(8)**.

472

473 Perus, I., and P. Fajfar (2014). Prediction of site factors by a non-parametric approach, *Earthquake*

474 *Engng Struct. Dyn.* **43** 1743–1761.

475

476 Rathje, E. M., W. J. Chang, K. H. , Stokoe, and B. R. Cox (2004). Evaluation of ground strain from  
477 in situ dynamic response, in *Proceeding of the 13th World Conference on Earthquake Engineering*,  
478 Vancouver, B.C., Canada. August 1 to 6, Paper No. 3099.

479

480 Régnier, J., H. Cadet, L.F. Bonilla, E. Bertand, and J. Semblat (2013). Assessing nonlinear behavior  
481 of soil in seismic site response: Statistical analysis on KiK-net strong motion data, *Bull. Seism. Soc.*  
482 *Am.* **103(3)** 1750-1770.

483

484 Rodriguez-Marek, A., G. A. Montalva, F. Cotton, and L. F. Bonilla (2011). Analysis of single-station  
485 standard deviation using the KiK-net data, *Bull. Seism. Soc. Am.* **101(3)** 1242-1258.

486

487 Rubinstein, J. L., and G. C. Beroza (2005). Depth constraints on nonlinear strong ground motion from  
488 the 2004 Parkfield earthquake, *Geophysical research letters* **32(14)**.

489

490 Sawazaki, K., H. Sato, H. Nakahara, and T. Nishimura (2009). Time-lapse changes of seismic  
491 velocity in the shallow ground caused by strong ground motion shock of the 2000 Western-Tottori  
492 earthquake, Japan, as revealed from coda deconvolution analysis, *Bull. Seism. Soc. Am.* **99(1)** 352-  
493 366.

494

495 Sleep, N. H. (2010). Nonlinear behavior of strong surface waves trapped in sedimentary basins, *Bull.*  
496 *Seism. Soc. Am.* **100(2)** 826-832.

497

498 Vucetic, M. (1994). Cyclic threshold shear strains in soils, *J. Geotech. Eng.* **120** 2208–2228

499

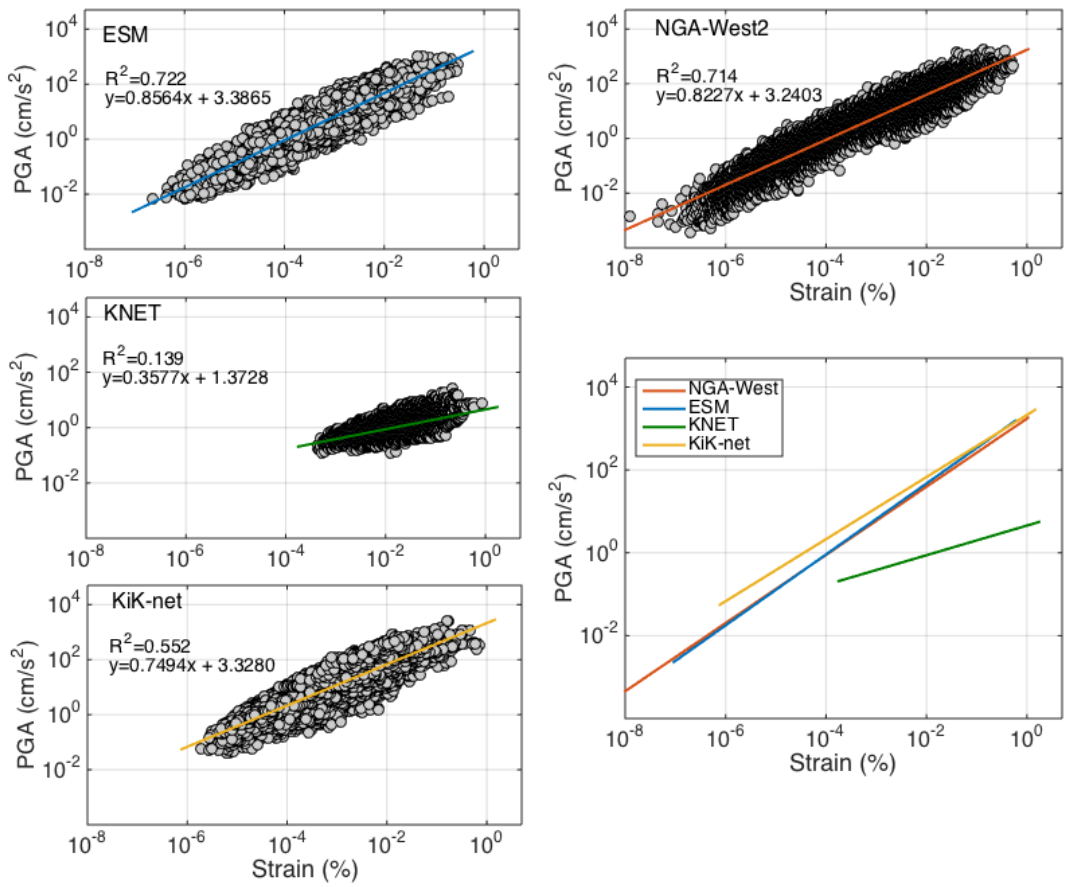
500 Zhao, J.X., J. Hu, F. Jiang, J. Zhou, Y. Zhang, X. An, M. Lu, and D. A. Rhoades (2015). Nonlinear  
501 site models derived from 1D analyses for ground-motion prediction equations using site class as the  
502 site parameter, *Bull. Seism. Soc. Am.* **105(4)** 2010–2022.

503

504

505

506

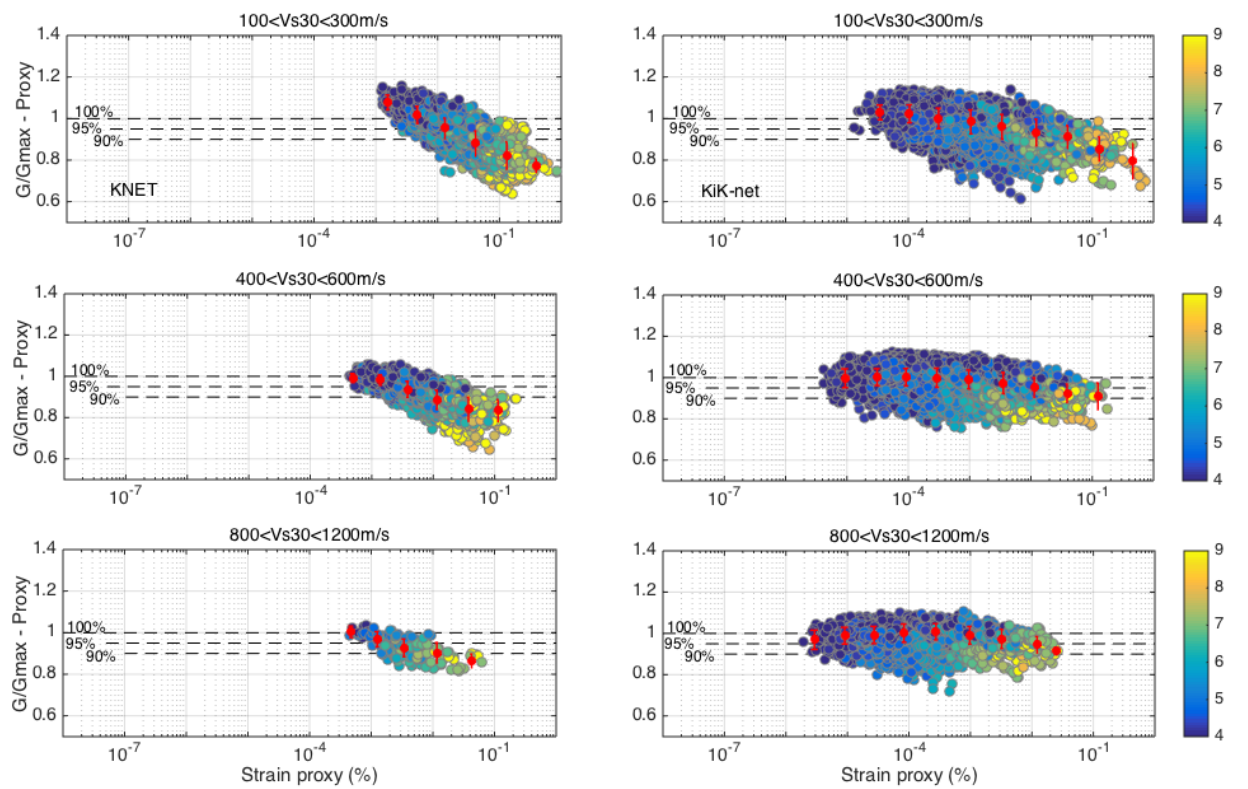
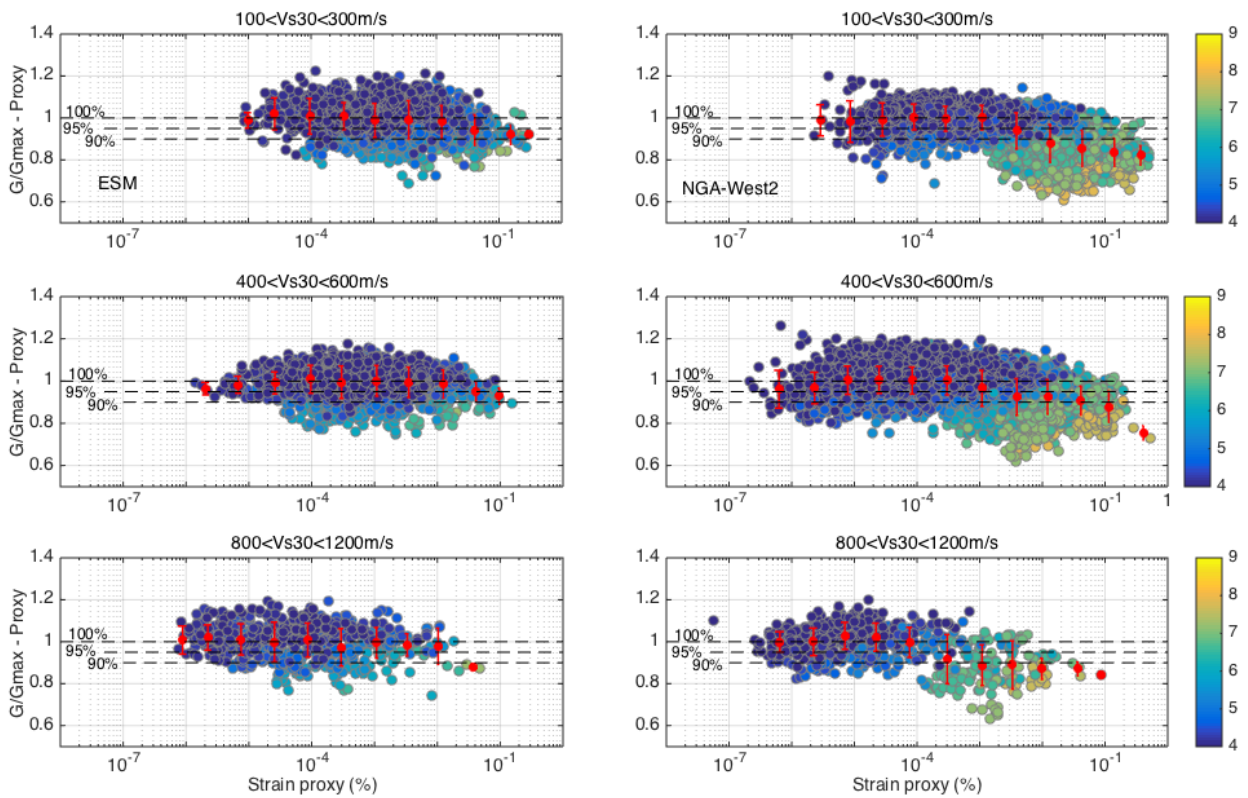


508

509

510 **Figure 1** – Data distribution, according to the deformation estimated by PGV/V<sub>s30</sub> for the four  
 511 databases used. Strain proxy is given as a percentage (see text for explanations). Best-fit linear  
 512 equations and coefficients of determination R<sup>2</sup> are given for all databases (lines).

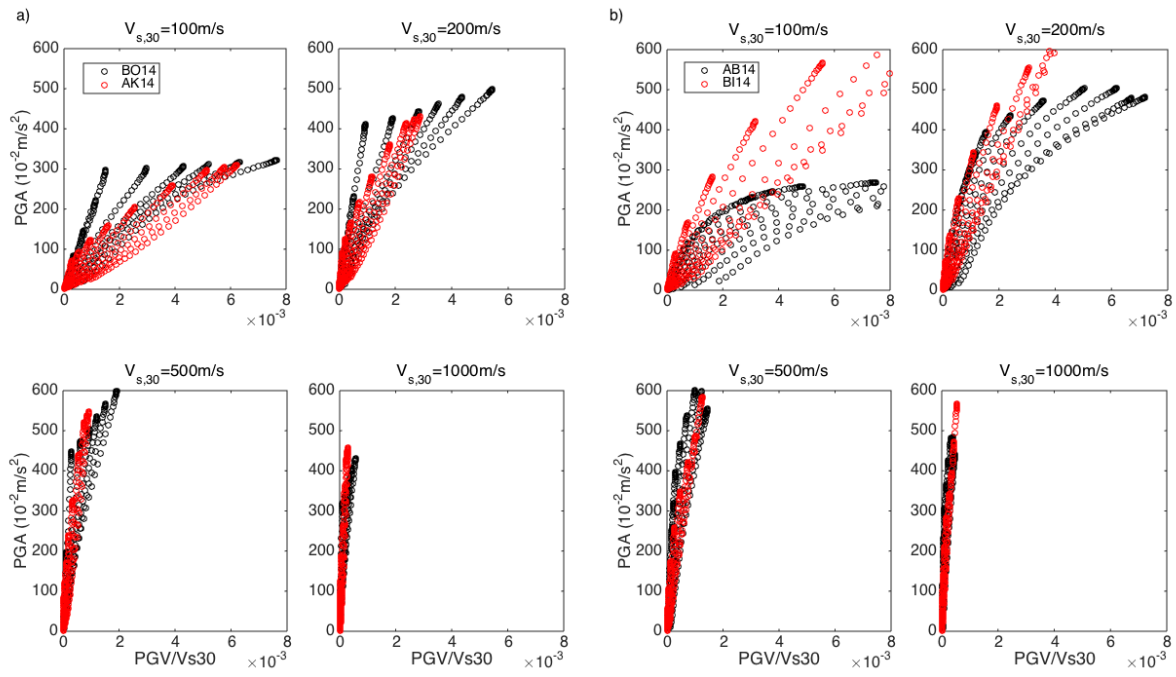
513



517 **Figure 2** – Modulus  $G$  variation according to the strain proxy calculated by Eq. 3 and 5, for three site  
 518 classes. The red symbols correspond to the average (+/- standard deviation) per strain proxy range

519 (see text). The color scale corresponds to magnitude. Horizontal dashed lines correspond to 100%,  
520 95% and 90% of the values of  $G/G_{\max}$ . a. ESM and NGA, b: K-NET and KiKNet.  
521  
522

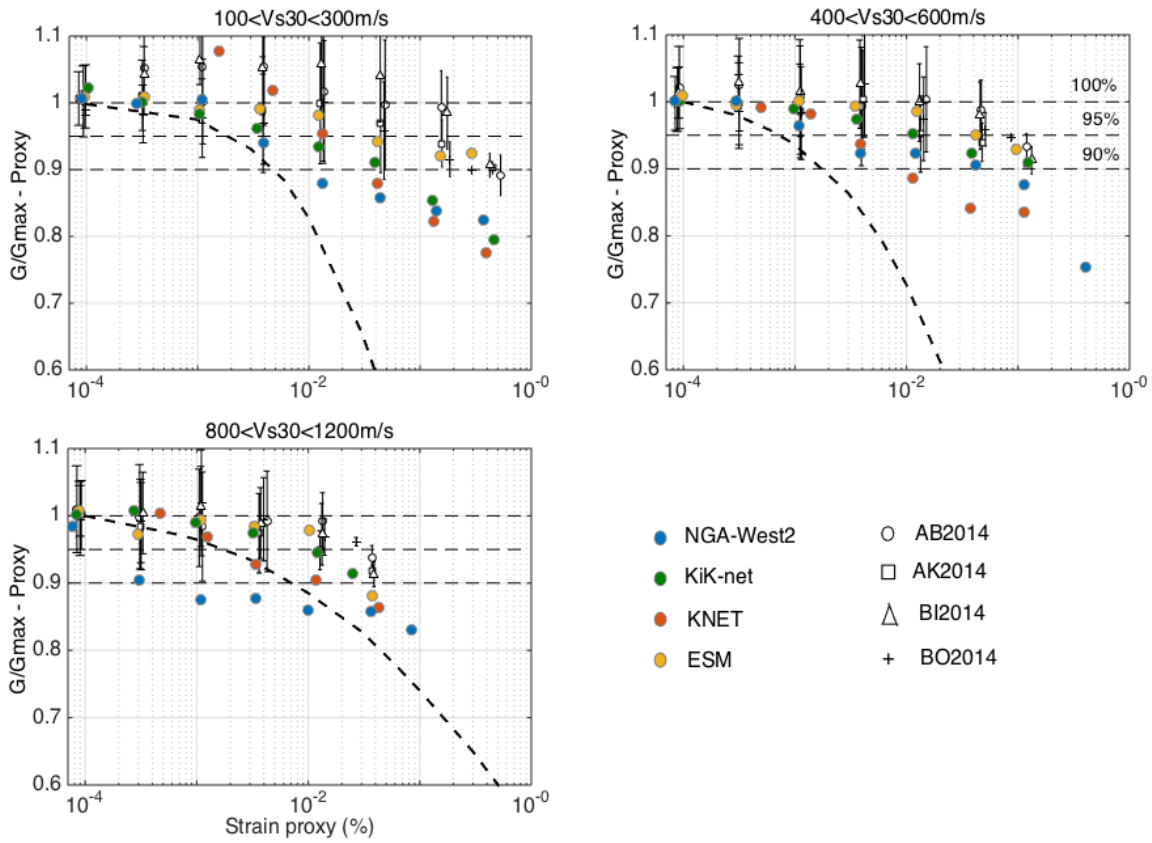




523

524 **Figure 3** – Predicted *PGA* as a function of the predicted deformation. Each dot corresponds to a  
 525 magnitude-distance pair for magnitudes between 4 and 8 (interval=0.5) and 50 distances between 0.1  
 526 and 300km. a) Boore et al. (2014) and Akkar et al. (2014). b) Abrahamson et al. (2014) and Bindi et  
 527 al. (2014).

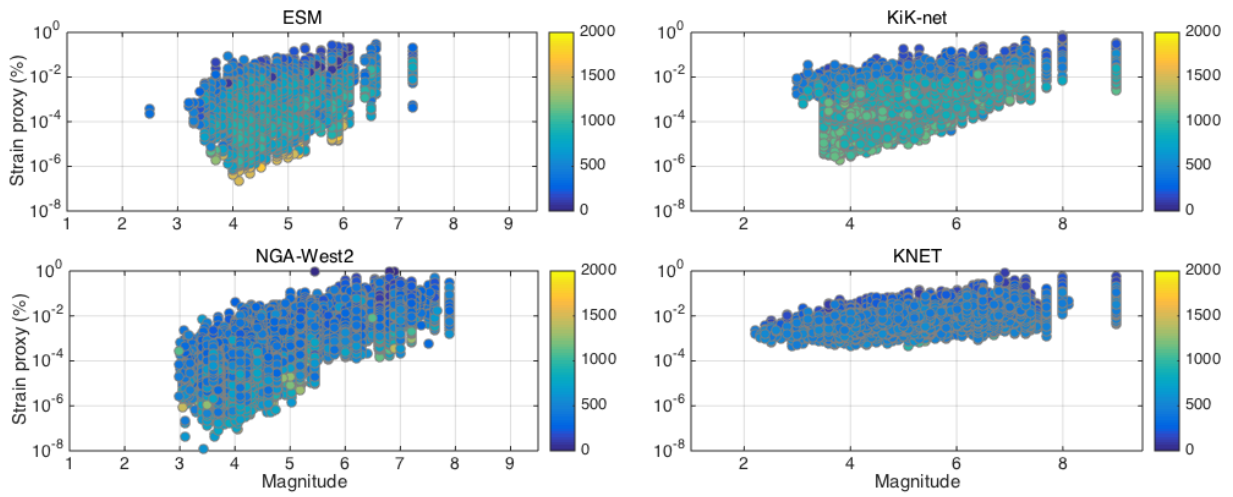
528



529

530 **Figure 4** – Comparison of predictions of nonlinearity characterized by the proxy  $G/G_{max}$  (Eq. 5) as  
 531 a function of the strain proxy ( $PGV/V_{s30}$ ) according to four GMPEs (AB2014: Abrahamson et al.,  
 532 2014; AK2014: Akkar et al., 2014; BI2014: Bindi et al., 2014; BO2014: Boore et al., 2014) on average  
 533 values from the four databases for three site classes, for strain proxies  $> 10^{-4}$  %. Thin horizontal  
 534 dashed lines correspond to 100%, 95% and 90% of the  $G/G_{max}$  values. Bold dashed lines are standard  
 535  $G-\gamma$  curves for clay (PI=15%), sand and rock-like soil from Zhao et al. (2015).

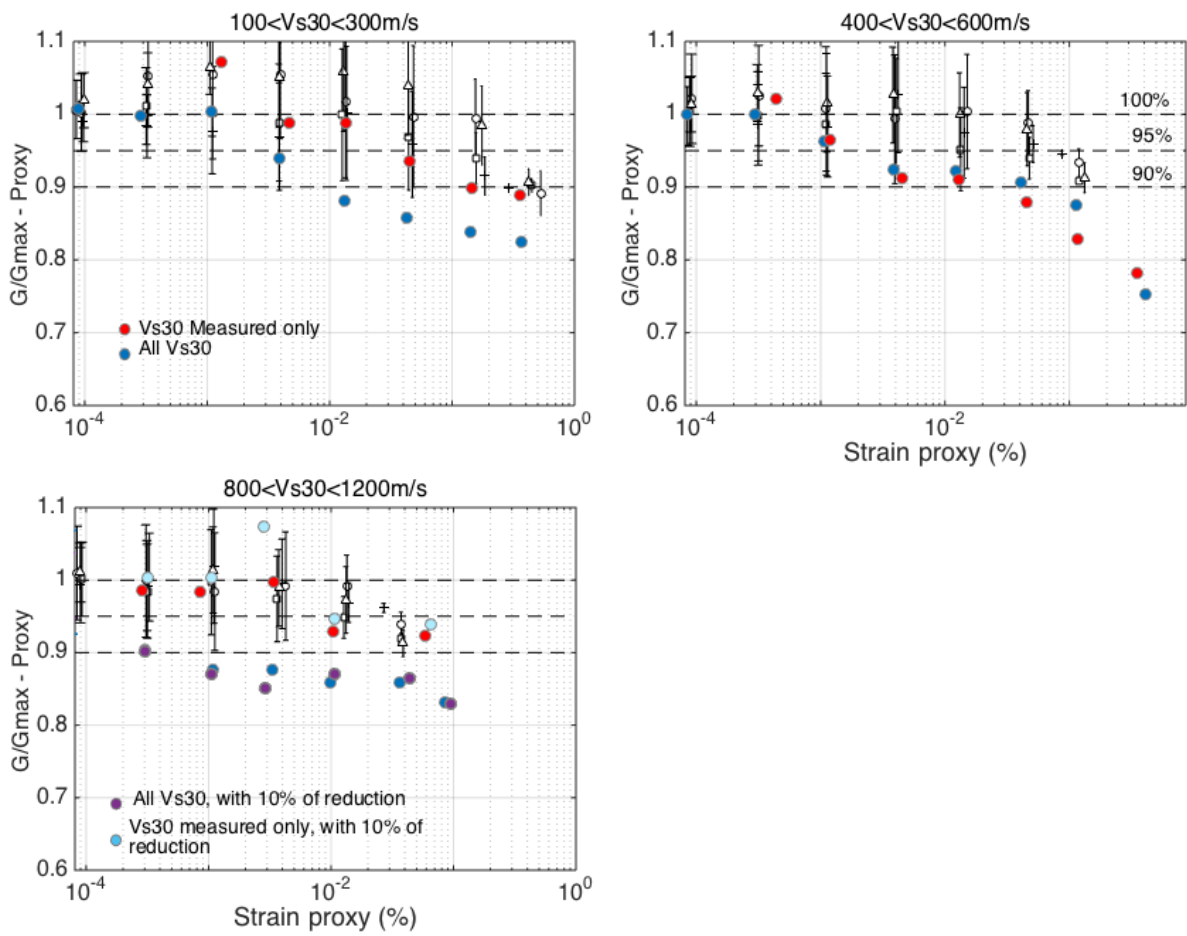
536



537

538 **Figure 5** – Soil shear deformation ( $PGV/V_{s30}$ ) as a function of earthquake magnitude. The color scale  
 539 indicates  $V_{s30}$ .

540



542

543 **Figure 6** – Same as Fig. 4 for NGA-West2 only, distinguishing measured  $V_{s30}$  values. For

544  $800 < V_{s30} < 1,200 \text{ m/s}$  sites, the  $V_{s30}$  values are also modified randomly by -10%.

545

546

547

548

549

550

551

552

553

554

555